Article

Elastohydrodynamic Performance of a Bio-Based, Non-Corrosive Ionic Liquid

Marcus Björling [1],* [ID]**, Scott Bair [2], Liwen Mu [3], Jiahua Zhu [3] and Yijun Shi [1]**

[1]   Division of Machine Elements, Department of Engineering Science and Mathematics, Luleå University of Technology, SE-97187 Luleå, Sweden; yijun.shi@ltu.se

[2]   Georgia Institute of Technology, Centre for High Pressure Rheology, G.W. Woodruff School of Mechanical Engineering, Atlanta, GA 30332-0405, USA; scott.bair@me.gatech.edu

[3]   Intelligent Composites Laboratory, Department of Chemical and Biomolecular Engineering, The University of Akron, Akron, OH 44325, USA; fujin.1234@163.com (L.M.); jzhu1@uakron.edu (J.Z.)

*   Correspondence: marcus.bjorling@ltu.se; Tel.: +46-920-491281

Abstract: To improve performance of machine components, lubrication is one of the most important factors. Especially for use in extreme environments, researchers look for other solutions rather than common lubricant base stocks like mineral oils or vegetable oils. One such example is ionic liquids. Ionic liquids have been defined as molten salts with melting points below 100 °C that are entirely ionic in nature, comprising both cationic and anionic species. The industrial use of ionic liquids is mostly as solvents, electrolytes, extractants and catalysts. In tribological applications, ionic liquids are mainly studied in boundary lubrication and in pure sliding contacts. In this work, the elastohydrodynamic performance of a bio-based, non-corrosive, [choline][L-proline] ionic liquid is evaluated in terms of pressure-viscosity response, film forming capability and friction. The results show a pressure-viscosity coefficient of below 8 GPa^{-1} at 25 °C, among the lowest reported for any ionic liquid. The ionic liquid generated up to 70% lower friction than a reference paraffin oil with a calculated difference in film thickness of 11%. It was also shown that this ionic liquid is very hygroscopic, which is believed to explain part of the low friction results, but also has to be considered in practical applications since the water content will influence the properties and thus the performance of the lubricant.

Keywords: Ionic liquid; EHL; friction; film thickness; bio-based; non-corrosive; pressure-viscosity; elastohydrodynamic

1. Introduction

Lubrication plays a vital part in the efficiency of machine components. Improved lubrication can significantly increase the efficiency of machine components. For use in extreme environments, researchers are looking for other solutions rather than conventional hydrocarbon based or mineral based oils. One such example are ionic liquids (ILs). ILs have been defined as molten salts with melting points below 100 °C that are entirely ionic in nature, comprising both cationic and anionic species. Other descriptions include non-aqueous ionic liquid, molten salt, liquid organic salt and fused salt [1]. ILs are widely used in several industrial applications such as electrolytes in electrochemistry, solvents, extractants and catalysts in organic synthesis since they possess excellent electrochemical stability, low volatility, large charge density, tunable polarity, high temperature stability etc. [2,3]. Some of these features make them interesting as lubricants and ILs have begun to gain attention for their tribological properties since 2001 [4]. Several researchers have shown that ILs demonstrate low wear and friction in steel-steel contacts [4–9], aluminium-steel contacts [4,10,11], nickel-steel contacts [12], copper-steel contacts [4] and ceramic-steel contacts [4,13]. Aside from potential problems

with corrosion and additive compatibility most ILs are significantly more expensive to manufacture compared to more common lubricants. Several researchers have therefore explored the use of ILs as lubricant additives [14–17] with promising results, although some of the interesting properties such as the low volatility of the pure liquid may be lost.

Lubrication is usually divided into three regimes; boundary, mixed and full film lubrication [18]. Most of the research articles focus on the performance of ionic liquids in boundary and mixed lubrication. Little research is available in literature concerning the performance of ILs in full film elasto hydrodynamic lubrication (EHL) [19,20]. EHL is found in for instance gears, rolling element bearings and cam followers, and it is of interest how ILs performs in this lubrication regime. Since most of these systems consist of steel surfaces it is important that the lubricant prevents corrosion. Several types of ILs have been shown to lead to corrosion of steels [21].

In this work, the pressure-viscosity response, film forming capacity and frictional behavior in full film elastohydrodynamic lubrication have been investigated for a protic, bio-based [choline][amino acid] IL. The study reports a pressure viscosity coefficient of below 8 GPa^{-1} at 25 $°$C, among the lowest reported for any ionic liquid. The friction measurements show up to 70% lower friction with the ionic liquid at very similar film thickness compared to the paraffin reference oil.

2. Overall Methodology

The following sections cover lubricants and test specimens. It also contains information about how the limiting-low-shear viscosities of the ionic liquid were measured and how this information was used to calculate pressure-viscosity coefficients. There is also a description of the experimental equipment for the film thickness measurements and how the measurements were performed. Finally, there is a description of how the friction measurements were conducted.

2.1. Lubricants and Test Specimens

The lubricant evaluated in this work is a protic, bio-based [choline] [L-proline] ionic liquid, see Figure 1 for the molecular structure. This green IL has earlier been evaluated in terms of non-corrosiveness, thermal degradation and boundary lubrication performance [22], in which it is denoted IL2. The synthesis of the IL was as follows: Choline hydroxide solution was added dropwise to equimolar proline amino acid with ice cooling. In the next step, the mixture was magnetically stirred at room temperature for 48 h. Afterwards, the water in the mixture was removed using a rotary evaporator at 60 $°$C. Finally, the IL was dried in vacuum for 48 h at 60 $°$C.
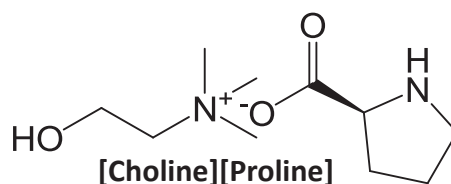

Figure 1. Molecular structure of [Choline] [Proline] ionic liquid.

An analytical grade paraffin oil from sigma-aldrich was used as a reference for the film thickness and friction tests. A fluid without additives was chosen to minimize additive effects on film thickness and friction. The refractive index of the lubricants were measured with an Abbe Refractometer, and the absolute viscosities were measured at 25 and 60 $°$C with a Bohlin CVO 100 rheometer. A concentric cylinder geometry was used with a 25 mm inner diameter and a 27 mm outer diameter. In each measurement, the shear rate was controlled at 20 s^{-1}.

The test specimens for the friction measurements in the ball on disk machine were produced in DIN 100Cr6 (AISI 52100) bearing steel and measured to a surface roughness, RMS of 20 nm for the balls and 25 nm for the disks, which gives a combined roughness of approximately 32 nm. The disk used

for the film thickness measurements is made from Pyrex glass and has an elastic modulus of 64 GPa, a poisons ratio of 0.2 and a surface roughness, RMS below 5 nm. The surface roughness measurements were conducted in a Wyko NT1100 optical profilometer system from Veeco. The measurements were performed using 10× magnification and 1× field of view. The balls are grade 20 with a 13/16 inch (20.63 mm) outer diameter and a hardness of about 60 HRC. The steel disks have a 4 inch (101.6 mm) outer diameter, a circumferential grind (before polish) and are through hardened to about 60 HRC.

2.2. Limiting Low Shear Measurements and Pressure-Viscosity Calculations

The limiting-low-shear viscosities of the [choline] [L-proline] IL were measured up to 350 MPa with a falling cylinder viscometer using a sinker which applies shear stress of 5.7 Pa. The measurements were conducted at the Center for High-Pressure Rheology at Georgia Institute of Technology following the procedure described in [23]. Because of the low shear stress used in these stress-controlled measurements, the viscosities may be considered to be the limiting-low-shear viscosities. Temperatures of 25, 50 and 90 °C were employed. The estimated uncertainties are 3% for viscosity, 0.5 °C for temperature and the greater of 1 MPa and 0.5% for pressure. Before the measurements, the viscometer cartridge was heated up to 150 °C and vacuum was applied to remove bubbles. This process also reduced the water content of the sample.

The pressure-viscosity coefficients based on the measured limiting-low-shear viscosities of the [choline] [L-proline] IL were calculated with the use of the McEwen model [24,25] for the following pressure-viscosity definitions: The conventional pressure-viscosity coefficient, α_0 the reciprocal asymptotic isoviscous pressure coefficient, α^* employed in Hamrock & Dowson film thickness formulas [26], and finally the general film-forming pressure-viscosity coefficient α_{film}. A more complete description of the different definitions of pressure-viscosity coefficients can be found elsewhere [27].

The Hamrock and Dowson [26] film thickness formula employs the reciprocal asymptotic isoviscous pressure coefficient, $\alpha^* = 1/p_{ia}$, as the pressure-viscosity coefficient.

$$p_{ia} = \int_0^\infty \frac{\mu(p=0)dp}{\mu(p)} \tag{1}$$

The 1952 McEwen model [24] can be written in terms of α^*:

$$\mu = \mu_0 \left(1 + \frac{\alpha^*}{q-1} p\right)^q, q > 1 \tag{2}$$

This model is widely used by laboratories which actually measure viscosity under pressure. See for example [28]. The McEwan model can also be used to obtain the conventional pressure-viscosity coefficient:

$$\alpha_0 = \left[\frac{d\ln\mu}{dp}\right]_{p=0} = \frac{\alpha^*}{\left(1 - \frac{1}{q}\right)}, q > 1 \tag{3}$$

The proper pressure-viscosity coefficient for film thickness [27] is:

$$\alpha_{film} = \frac{1 - exp(-3)}{p_i(3/a^*)} \tag{4}$$

with

$$p_i(p) = \int_0^p \frac{\mu(p=0)d\hat{p}}{\mu(\hat{p})} \tag{5}$$

when Blok's integral above converges. In terms of the McEwen parameters it is:

$$\alpha_{film} = \frac{a \times (1 - exp(-3))}{1 - \left[1 + \frac{3}{q-1}\right]^{1-q}}$$

(6)

Here, p is the pressure, p_{ia} is the asymptotic isoviscous pressure, q an exponent, μ is the limiting low-shear viscosity at local pressure and μ_0 is the low shear viscosity at $p = 0$.

2.3. Film Thickness Measurements

The film thickness measurements were performed in the same test rig as the friction measurements, as described in Section 2.4, but modified to allow for optical measurements of the film thickness, as shown in Figure 2. The lubricant is situated in a container in which the ball is rotating, and a pump system is used to keep this container filled with lubricant to ensure fully flooded conditions. Heaters are placed in both the smaller oil container where the ball is placed, but also in the bigger lubricant supply below to enable heating of the lubricants. The steel disc is substituted by a Pyrex glass disk with a chromium semi-reflecting coating acting as a beam splitter, and an optical microscope is attached on top to allow study of the film formed between the steel ball and the glass disk. A beam of white light is directed through the glass disc into the contact where a part is reflected back by the chromium layer, while the rest passes through the lubricant film before being reflected back by the steel ball. There will be a phase shift of the light due to the difference in optical path length for the light reflected in the beam splitter, and the light reflected at the ball surface. This can be used to calculate the film thickness. See for instance refs [29,30] for more information on optical interferometry and its use for lubricant and grease film thickness measurements. Several different methods have been proposes for the translation of optical phase differences into film thickness [31–33], where the method described by Hartl et al. [33] is used in the present work.
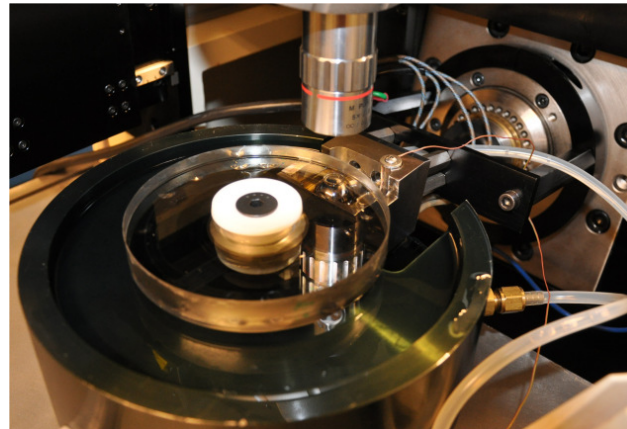

Figure 2. Wedeven Associates Machines ball on disc test apparatus with optical interferometry setup.

The ball on disk test device was used to measure film thickness of the two lubricants at two different temperatures; 25 and 60 °C. All measurements were conducted at a condition as close as possible to pure rolling. Before starting the experiments for each lubricant, the test device was warmed up to the desired operating temperature for approximately 60 min with lubricant circulating over both ball and disk to ensure thermal stability. At the start of each test cycle the entrainment speed is set to a reasonably high value to ensure a condition of full film lubrication when a load of 27 N, which corresponds to a maximum Hertzian pressure of 0.5 GPa is applied. The entrainment speed is then reduced to a limit where the film thickness is around 100 nm, and the measurement series is started. The speed is gradually increased to the point where the intensity of the interference is too low to get an estimation of the film thickness, or to the point where oil splash is so great that the loss of lubricant is too high.

An approximation of the pressure-viscosity coefficient, alpha of each lubricant at both 25 and 60 °C was calculated by the use of the Hamrock and Dowson equation for central film thickness [26]:

$$H_c = 2.69 U^{0.67} G^{0.53} W^{-0.067} (1 - 0.61 e^{-0.73k}) \tag{7}$$

where H_c is the central film thickness, U the dimensionless speed parameter, G the dimensionless material parameter, W the dimensionless load parameter and k the ellipticity parameter. Since all of these are known except the pressure-viscosity coefficient, an approximation of this parameter can be computed by use of a least square fit to match each film thickness in a measurement series as close as possible. A thorough description in the use of optical interferometry and film thickness equation to assess pressure-viscosity coefficients is given elsewhere [34].

2.4. Friction Measurements

The experiments were carried out with a Wedeven Associates Machine (WAM) 11, ball on disk test device. The lubricant is supplied at the center of the disk in an oil dispenser that distributes the lubricant across the disk surface. The lubricant is circulated in a closed loop from the oil bath, through a peristaltic pump to the oil dispenser at the center of the disk. The peristaltic pump is delivering approximately 180 mL/min. Three thermocouples are used in the test setup, one located in the oil bath, one in the outlet of the oil supply, and one trailing in the oil film close to the inlet region of the ball on disk contact. A more thorough description of the test rig and its features is presented in previous work [35].

The ball on disk test device was used to generate friction data from a series of tests under different operating conditions. Two different entrainment speeds were used; 1 and 3 m/s. The slide to roll ratio (SRR) were varied between 0.002 and 1.05. SRR is defined as the ball surface speed minus the disk surface speed, divided by the entrainment speed. All tests in this investigation were hence conducted with the ball having a higher surface speed than the disk. Both ball and disk specimens were cleaned with heptane and ethyl alcohol before starting the experiments for each of the test cases. The tests were performed with two different loads; 100 and 300 N, which corresponds to a maximum Hertzian pressure of 1.25 and 1.95 GPa respectively. The tests were performed at a temperature of 40 °C. Before starting the experiments for each test case, the test device was warmed up to the desired operating temperature for approximately 60 min with lubricant circulation over both ball and disk to ensure thermal stability. When a stable temperature was reached, a 100 or 300 N load was applied and the machine was calibrated for pure rolling by adjusting spindle angle and positioning of the ball to ensure a condition of no spinning. These settings were then held constant for 20 min to ensure a mild run-in. Subsequently, the test cycle was started, wherein the load and entrainment speed were kept at constant values, and slide to roll ratio were varied from the lowest to the highest value. The temperature of the oil bulk and fluid adhered to the disk surface was typically deviating less than ± 1 °C from the target temperature of 40 °C during testing. A summary of the test conditions is found in Table 1. All tests were performed five times to ensure repeatability.

Table 1. Frictiontest conditions.

Lubricant	IL and paraffin
Temperature	40 °C
Contact load, F	100 and 300 N
Maximum hertzian pressure	1.25 and 1.95 GPa
Entrainment speed, U_e	1 and 3.14 m/s
Slide to Roll Ratio, SRR	0.0002 to 1.05

3. Results and Discussion

The results from the pressure-viscosity measurements of [Choline] [Proline] at three different temperatures are shown in Figure 3. The curves in the figure are from the improved

Yasutomi correlation, a pressure modification of the Williams-Landel-Ferry model for temperature dependence [36]. The parameters for the improved Yasutomi correlation can be seen in Table 2.
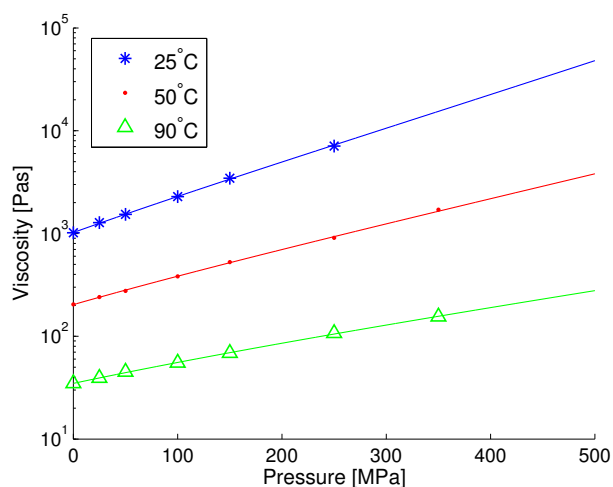

Figure 3. Viscosity pressure curves for [Choline] [Proline] at various temperatures.

Table 2. Parameters of the Improved Yasutomi correlation for [Choline] [Proline].

μ_g [Pas]	10^{12}
T_{g0} [°C]	-76.20
A_1 [°C]	111.47
A_2 [GPa^{-1}]	0.5664
b_1 [GPa^{-1}]	3.240
b_2	-0.1422
C_1	16.625
C_2 [°C]	39.14
Std. Dev	1.5%

Based on these pressure-viscosity measurements, pressure-viscosity coefficients by three different definitions were calculated based on the McEwen model [25]. The results are shown in Table 3. These definitions and calculations assume that Blok's integral will converge for the liquid, a fact not in evidence. These measured values are substantially lower than pressure-viscosity coefficients usually measured for common hydrocarbon oils that are usually in the range of 15–25 Gpa^{-1} at room temperature [23,37,38]. The pressure-viscosity coefficients of [Choline] [Proline] are also compared to some other ionic liquids [39–45], summarized in [46] and shown in Table 4. In this comparison, [Choline] [Proline] IL has the lowest pressure-viscosity response of the investigated ILs. Other researchers have found even lower α_{film} for [C$_2$C$_1$Im][C$_2$SO$_4$] [47]. The large variation in pressure-viscosity coefficients between different kinds of fluids are connected to the differences in molecular structure. The literature is surprisingly sparse in studies on this relationship. Bair [48] has shown that the general trend is that the pressure-viscosity coefficient is increased when going from a few long branches to many short branches. An example is given in Figure 4 where the pressure viscosity response of two isomers of dodecane is shown.
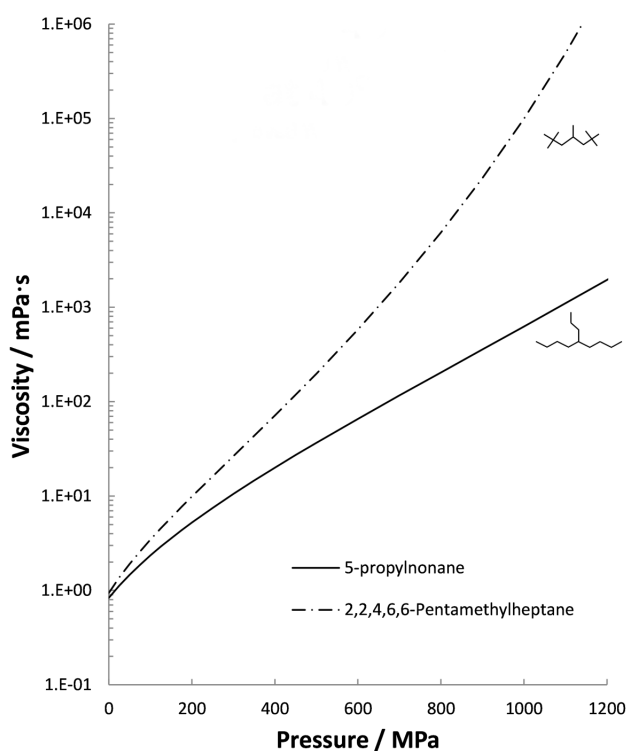
Figure 4. Viscosity pressure curves for two Isomers of Dodecane @ 40 °C.

Table 3. Pressure-viscosity coefficients for [Choline] [Proline].

T [°C]	25	50	90
α_0 [GPa^{-1}]	8.92	6.76	4.73
α^* [GPa^{-1}]	7.65	5.81	4.08
α_{film} [GPa^{-1}]	7.96	6.05	4.25

Table 4. Comparison of pressure-viscosity coefficients.

	α^* [GPa^{-1}] 25 °C	α^* [GPa^{-1}] 50 °C	α_{film} [GPa^{-1}] 25 °C	α_{film} [GPa^{-1}] 50 °C
[Choline][Proline]	7.7	5.8	8.0	6.1
[C$_4$C$_1$im]BF$_4$	9.9	7.8	10.1	8.2
[C$_4$C$_1$im]PF$_6$	13.2	10.5	13.5	10.9
[C$_4$C$_1$im]Tf$_2$N	10.7	8.6	11.1	9.1
[C$_6$C$_1$im]Pf$_6$	13.7	11.1	14.1	11.6
[C$_6$C$_1$im]Tf$_2$N	9.5	8.6	9.5	8.5
[C$_8$C$_1$im]Bf$_4$	11.1	9.0	11.7	9.6
[C$_8$C$_1$im]Pf$_6$	13.3	11.1	13.9	11.7

Here it is clear that the highly branched 2,2,4,6,6-Pentamethylheptane has a significantly higher pressure viscosity response than 5-propylnonane. The same is true when going from linear to cyclic and then to polycyclic structures [48]. It has also been discussed that an increase in side chain will increase the pressure viscosity coefficient [46]. Generally, this seem to hold when observing the values in Table 3. The ILs having a [C$_4$C$_1$im] cation seem to scale in pressure-viscosity in the order of the branch densities of the anions BF$_4$, Tf$_2$N and PF$_6$. In general, an increase in chain length of the cation with the same anion also increases the pressure viscosity coefficient for the ILs in Table 3. The [Choline][Proline] with a lower branch density than the ILs in Table 3 therefore has lower-pressure viscosity coefficients.

A lower pressure-viscosity coefficient means that the viscosity will not increase as much with pressure compared to a higher pressure-viscosity fluid. This has primarily two effects. The first one

is that the film thickness generated will not be as large, since it is dependent on the viscosity of the lubricant in the inlet region of the contact. The second effect is that the effective viscosity inside of the high pressure region of the contact will be lower, which in turn will lead to a lower coefficient of friction in full film conditions. However, since a lower pressure-viscosity coefficient leads to lower film thicknesses, the transition from full film to mixed and boundary lubrication will occur at higher entrainment speeds or for lower roughness levels, which in turn will increase friction and wear. Furthermore, a low pressure-viscosity coefficient is often connected to a low limiting shear stress of the lubricant, which is also beneficial for low friction coefficients [37]. The values for α^* are vastly different for those derived from viscosity in Table 3 and those derived from film thickness. This is a well-known issue for EHL [49]. The classical EHL film thickness formulas often require values of the pressure-viscosity coefficients that cannot be measured in a viscometer with the usual definitions. This issue can only be resolved when EHL employs real viscosity in calculations.

The present investigation shows that [Choline] [Proline] is a very hygroscopic IL. A sample of the IL was left in open atmosphere at 25 °C and a relative humidity of approximately 15 % for 180 h and the water content was measured at certain intervals. The results can be seen in Figure 5. The water content in the IL increased to almost 10 wt % in 24 h and then leveled out at a level slightly below 15 wt %. Since this IL was shown to be highly hygroscopic it was decided that the film thickness and friction tests would be performed at the saturated level of water content of slightly below 15 wt %.
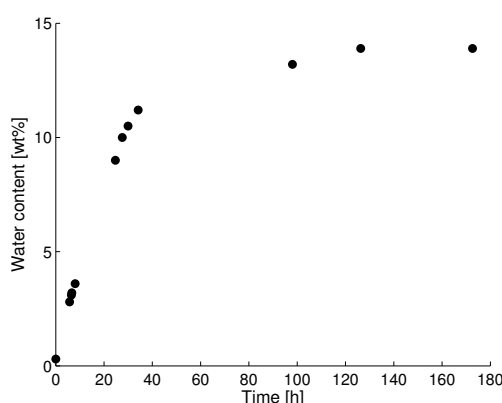

Figure 5. Water content increase in [Choline] [Proline] at relative humidity of 15%.

The viscosity of the water containing IL and the reference paraffin oil was measured in a Bohlin CVO 100 rheometer at 25, 40 and 60 °C. The results are shown in Table 5. Here the refractive indexes used in the optical film thickness measurements are also presented.

Figure 6 shows the central film thickness of [Choline] [Proline] containing slightly less than 15 wt % water and the paraffin oil at 25 and 60 °C at 0.5 GPa of pressure. The film thickness for the IL is only slightly higher than for the paraffin oil despite the IL having significantly higher viscosity. By calculating the pressure-viscosity coefficient of the lubricants at the measured temperatures by use of an analytical film thickness equation gives pressure-viscosity values for the IL that is significantly lower than the paraffin. The values are presented in Table 5. It should be kept in mind that assessment of pressure-viscosity coefficients from film thickness measurements may not be the most precise method, and could also be erroneous should inlet shear thinning occur [49,50]. However, the pressure-viscosity values presented in Table 3 that are based on the falling cylinder viscometer results at high pressure confirms that the [Choline] [Proline] has a much lower pressure-viscosity than conventional hydrocarbon oils and that this is the reason to the comparatively low film thickness results shown in Figure 6.

Table 5. Data for test lubricants.

Lubricant	Paraffin	Ionic Liquid
Refractive index	1.47	1.46
Dynamic viscosity @ 25 °C [mPas]	93	227
Dynamic viscosity @ 40 °C [mPas]	46	92
Dynamic viscosity @ 60 °C [mPas]	21	37
α^*@ 25 °C [GPa^{-1}]	20.2	11.2
α^*@ 60 °C [GPa^{-1}]	17.6	9.7
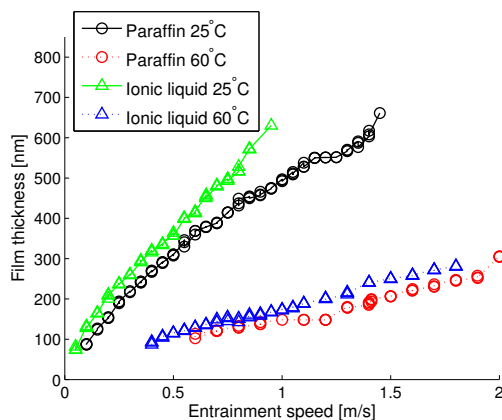
Figure 6. Central film thickness measurements for Paraffin and [Choline] [Proline] at 25 and 60 °C at 0.5 GPa of pressure. [Choline] [Proline] had a water content of slightly below 15 wt %.

The results from the friction measurements at the lower pressure of 1.25 GPa are shown in Figure 7. The friction coefficient for the IL is substantially lower than the friction coefficient for the paraffin oil at both entrainment speeds.
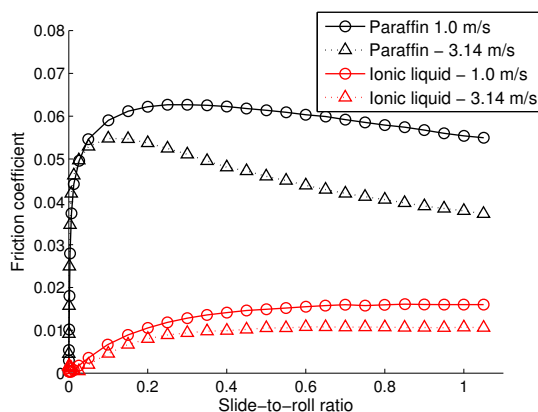
Figure 7. Friction measurements for Paraffin and [Choline] [Proline] at 40 °C and 1.25 GPa. [Choline] [Proline] had a water content of slightly below 15 wt %.

In Figure 8 the results from the friction measurements performed at 1.95 GPa of pressure are shown. Even here the friction coefficient for the IL is considerable lower than the friction coefficient for the paraffin oil at both entrainment speeds and both pressure levels.
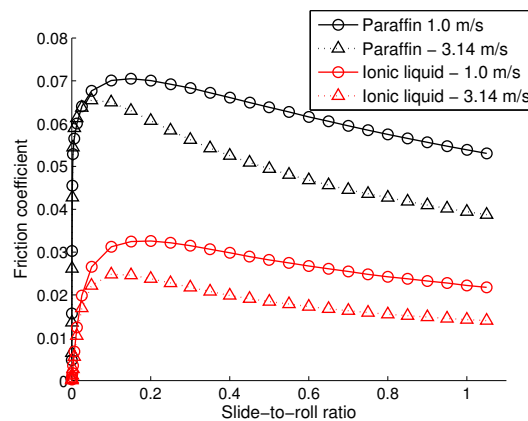
Figure 8. Friction measurements for Paraffin and [Choline] [Proline] at 40 °C and 1.95 GPa. [Choline] [Proline] had a water content of slightly below 15 wt %.

The Hamrock & Dowson central and minimum film thickness was calculated for the conditions of the friction tests with the lubricant parameters given in Table 5, and pressure-viscosity coefficients linearly interpolated to 19.04 GPa^{-1} for paraffin and 10.28 GPa^{-1} for the IL. The results are shown in Table 6.

Table 6. Hamrock & Dowson central and minimum film thickness for friction tests.

P [GPa]	U_e [m/s]	H_c Paraffin [nm]	H_c IL [nm]	H_{min} Paraffin [nm]	H_{min} IL [nm]
1.95	1	242	271	136	158
1.95	3.14	520	584	297	344
1.25	1	264	297	150	174
1.25	3.14	568	638	327	379

Evidently, all tests were performed in full film lubrication since the minimum film thickness for both lubricants at all combinations of speeds and pressures were significantly higher than the combined roughness of the specimens. It is however remarkable that the difference in friction between the IL and the paraffin is significant while the difference in film thickness is not that pronounced. At the pressure of 1.25 GPa and 1 m/s in entrainment speed, the friction coefficient is up to 70% lower for the IL compared to the paraffin oil. At the same entrainment speed, the calculated difference in film thickness is approximately 11%.

Another hygroscopic lubricant that generated low friction in full film elastohydrodynamic lubrication is glycerol and its aqueous solutions [51]. Here, it was seen that increasing water content would reduce friction up to a certain level where the friction coefficient started to increase with even higher water content. It was hypothesized that the increase in water content would reduce viscosity in the high pressure region of the contact and this reduce friction. At the same time, increased water content would also reduce film thickness due to lower viscosity in the inlet region of the contact. This would lead to higher risk of asperity interactions and thus increase friction when the film is no longer thick enough to fully separate the surfaces. This would explain the friction increase at higher levels of water content. Other researchers have also shown some evidence that in the case of glycerol lubrication, water has been produced inside the high pressure contact thus contributing to the low friction [52]. Whether a similar reaction is taking place for the IL studied in this work has not been investigated. While for both glycerol and the IL studied in this work, the hygroscopic properties and the water content may help to reduce friction, it also makes the lubricants more challenging to use since the water content will influence both film forming capacity and friction properties.

4. Conclusions

The purpose of this work was to investigate the full film elastohydrodynamic performance of a [Choline] [Proline] ionic liquid in terms of pressure-viscosity response, film formation and friction behaviour. The limiting low shear viscosity was measured up to 350 MPa for different temperatures. From these measurements, the McEwen model was used to calculate the pressure-viscosity coefficients of the fluid. The resulting pressure-viscosity coefficients of below 8 GPa^{-1} at 25 °C are among the lowest reported for any ionic liquid, and assumed to be a result of a low branch density. [Choline] [Proline] was also shown to be very hygroscopic where the water content increased from nearly 0 wt % to around 10 wt % in 24 h in room temperature with a relative humidity of 15%. Film thickness and friction measurements were conducted in a ball on disk machine at 1.25 and 1.95 GPa with the ionic liquid having a water content slightly below 15 wt % and a paraffin oil as a reference. The ionic liquid showed up to 70% lower friction than the paraffin oil with a calculated difference in film thickness of 11%. The [Choline] [Proline] has the potential of providing low friction in elastohydrodynamic lubrication when used in for instance gear or rolling element bearings. However, the hygroscopic properties must be considered depending on the practical application. For use in space applications or applications where water content can be carefully controlled this IL may be a very interesting alternative.

Author Contributions: Marcus Björling designed and performed most of the measurements and analysis and wrote the manuscript. Scott Bair designed and performed the high pressure rheological measurements and the connected pressure-viscosity calculations. Liwen Mu and Jiahua Zhu synthesized the lubricants and were involved in interpreting the results. Yijun Shi conceived the project, helped with some of the experimental work and was involved in the interpretation of the results. All authors have given approval to the final version of the manuscript.

Conflicts of Interest: The authors declare no conflicts of interest.

Abbreviations

The following abbreviations are used in this manuscript:

EHL　　　Elasto hydrodynamic lubrication
HRC　　　Rockwell hardness
IL　　　　Ionic liquid
RMS　　　Root mean square
SRR　　　Slide to roll ratio
WAM　　　Wedeven Associates Machine

Nomenclature

α^*　　　Reciprocal asymptotic isoviscous pressure-viscosity coefficient [Pa^{-1}]
α_0　　　Conventional or initial pressure-viscosity coefficient [Pa^{-1}]
α_{film}　　General film forming pressure-viscosity coefficient [Pa^{-1}]
μ　　　　Limiting low shear viscosity at local pressure [Pa s]
μ_0　　　Low-shear viscosity at $p = 0$ [Pa s]
a　　　　Semimajor axis of contact ellipse
b　　　　Semiminor axis of contact ellipse
E　　　　Modulus of elasticity [GPa]
E'　　　　Effective elastic modulus, $E' = 2[(1 - v_1^2)/E_1 + (1 - v_2^2)/E_2]^{-1}$
F　　　　Normal applied load [N]
G　　　　Dimensionless material parameter, $G = \alpha^* E'$
H_c　　　Hamrock and Dowson central film thickness [m]
H_{min}　　Hamrock and Dowson minimum film thickness [m]
k　　　　Ellipticity parameter, a/b
p　　　　Pressure [Pa]
p_{ia}　　　Asymptotic isoviscous pressure [Pa]

q	Exponent
R_x	Effective radius [m]
U	Dimensionless speed parameter $U = U_e\mu_0/E'R_x$
U_e	Entrainment speed [m/s]
v	Poisson ratio
W	Dimensionless load parameter $W = F/(E'R_x^2)$

References

1. Welton, T. Room-temperature ionic liquids: Solvents for synthesis and catalysis. *Chem. Rev.* **1999**, *99*, 2071–2084.
2. Fedorov, M.V.; Kornyshev, A.A. Ionic liquids at electrified interfaces. *Chem. Rev.* **2014**, *114*, 2978–3036.
3. Hallet, J.P.; Welton, T. Room-temperature ionic liquids: Solvents for synthesis and catalysis. 2. *Chem. Rev.* **2011**, *111*, 3508–3576.
4. Ye, C.; Liu, W.; Chen, Y.; Yu, L. Room-temperature ionic liquids: A novel versatile lubricant. *Chem. Commun.* **2001**, *21*, 2244–2245.
5. Xia, Y.; Wang, S.; Zhou, F.; Wang, H.; Lin, Y.; Xu, T. Tribological properties of plasma nitrided stainless steel against SAE52100 steel under ionic liquid lubrication condition. *Tribol. Int.* **2006**, *39*, 635–640.
6. García, A.; González, R.; Battez, A.H.; Viesca, J.; Monge, R.; Fernández-González, A.; Hadfield, M. Ionic liquids as a neat lubricant applied to steel-steel contacts. *Tribol. Int.* **2014**, *72*, 42–50.
7. Sánchez, F.L.; Otero, I.; López, E.R.; Fernández, J. Tribological properties of two bis(trifluoromethylsulfonyl) imide-based ionic liquids on steel-steel contact. *Tribol. Trans.* **2014**, *57*, 637–646.
8. Nyberg, E.; Respatiningsih, C.Y.; Minami, I. Molecular design of advanced lubricant base fluids: Hydrocarbon-mimicking ionic liquids. *RSC Adv.* **2017**, *7*, 6364–6373.
9. Nyberg, E.; Mouzon, J.; Grahn, M.; Minami, I. Formation of boundary film from ionic liquids enhanced by additives. *Appl. Sci.* **2017**, *7*, doi:10.3390/app7050433.
10. Qu, J.; Blau, P.J.; Dai, S.; Luo, H.; Meyer, H.M.; Truhan, J.J. Tribological characteristics of aluminum alloys sliding against steel lubricated by ammonium and imidazolium ionic liquids. *Wear* **2009**, *267*, 1226–1231.
11. Somers, A.E.; Khemchandani, B.; Howlett, P.C.; Sun, J.; Macfarlane, D.R.; Forsyth, M. Ionic liquids as antiwear additives in base oils: Influence of structure on miscibility and antiwear performance for steel on aluminum. *ACS Appl. Mater. Interfaces* **2013**, *5*, 11544–11553.
12. Xia, Y.; Wang, L.; Liu, X.; Qiao, Y. A comparative study on the tribological behavior of nanocrystalline nickel and coarse-grained nickel coatings under ionic liquid lubrication. *Tribol. Lett.* **2008**, *30*, 151–157.
13. Liu, W.; Ye, C.; Chen, Y.; Ou, Z.; Sun, D.C. Tribological behavior of sialon ceramics sliding against steel lubricated by fluorine-containing oils. *Tribol. Int.* **2002**, *35*, 503–509.
14. Monge, R.; González, R.; Battez, A.H.; Fernández-González, A.; Viesca, J.L.; García, A.; Hadfield, M. Ionic liquids as an additive in fully formulated wind turbine gearbox oils. *Wear* **2015**, *328–329*, 50–63.
15. Fernandes, C.M.C.G.; Battez, A.H.; González, R.; Monge, R.; Viesca, J.L.; García, A.; Martins, R.C.; Seabra, J.H. Torque loss and wear of FZG gears lubricated with wind turbine gear oils using an ionic liquid as additive. *Tribol. Int.* **2015**, *90*, 306–314.
16. Jiménez, A.E.; Bermúdez, M.D.; Carrión, F.J.; Martínez-Nicolás, G. Room temperature ionic liquids as lubricant additives in steel-aluminium contacts: Influence of sliding velocity, normal load and temperature. *Wear* **2006**, *261*, 347–359.
17. Taher, M.; Shah, F.U.; Filippov, A.; de Baets, P.; Glavatskih, S.; Antzutkin, O.N. Halogen-free pyrrolidinium bis(mandelato)borate ionic liquids: Some physicochemical properties and lubrication performance as additives to polyethylene glycol. *RSC Adv.* **2014**, *58*, 30617–30623.
18. Björling, M.; Habchi, W.; Bair, S.; Larsson, R.; Marklund, P. Towards the true prediction of EHL friction. *Tribol. Int.* **2013**, *66*, 19–26.
19. Mordukhovich, G.; Qu, J.; Howe, J.Y.; Bair, S.; Yu, B.; Luo, H.; Smolenski, D.J.; Blau, P.J.; Bunting, B.G.; Dai, S. A low-viscosity ionic liquid demonstrating superior lubricating performance from mixed to boundary lubrication. *Wear* **2013**, *301*, 740–743.
20. Shi, Y.; Larsson, R. Non-corrosive and biomaterials protic ionic liquids with high lubricating performance. *Tribol. Lett.* **2016**, *63*, doi:10.1007/s11249-016-0692-9.
21. Minami, I. Ionic liquids in tribology. *Molecules* **2009**, *14*, 2286–2305.

22. Mu, L.; Shi, Y.; Guo, X.; Ji, T.; Chen, L.; Yuan, R.; Brisbin, L.; Wang, H.; Zhu, J. Non-corrosive green lubricants: Strengthened lignin-[choline][amino acid] ionic liquids interaction via reciprocal hydrogen bonding. *RSC Adv.* **2015**, *5*, 66067–66072.

23. Bair, S.; Qureshi, F. Accurate measurements of pressure-viscosity behavior in lubricants. *Tribol. Trans.* **2002**, *45*, 390–396.

24. McEwen, E. The effect of variation of viscosity with pressure on the load-carrying capacity of the oil film between gear-teeth. *J. Inst. Pet.* **1952**, *38*, 646–672.

25. Bair, S. Pressure-viscosity response in the inlet zone for quantitative elastohydrodynamics. *Tribol. Int.* **2016**, *97*, 272–277.

26. Hamrock, B.J.; Dowson, D. Isothermal elastohdrodynamic lubrication of point contacts: Part 3—Fully flooded results. *J. Lubr. Technol.* **1977**, *99*, 264–276.

27. Bair, S.; Liu, Y.; Wang, Q.J. The pressure-viscosity coefficient for Newtonian EHL film thickness with general piezoviscous response. *J. Tribol.* **2006**, *128*, 624–631.

28. Caudwell, D.R.; Trusler, J.P.M.; Vesovic, V.; Wakeham, W.A. Viscosity and density of five hydrocarbon liquids at pressures up to 200 MPa and temperatures up to 473 K. *J. Chem. Eng. Data* **2008**, *54*, 359–366.

29. Johnston, G.J.; Wayte, R.; Spikes, H.A. The measurement and study of very thin lubricant films in concentrated contacts. *Tribol. Trans.* **1991**, *34*, 187–194.

30. Cousseau, T.; Björling, M.; Graca, B.; Campos, A.; Seabra, J.; Larsson, R. Film thickness in a ball-on-disc contact lubricated with greases, bleed oils and base oils. *Tribol. Int.* **2012**, *53*, 53–60.

31. Gustafsson, L.; Höglund, E.; Marklund, O. Measuring lubricant film thickness with image analysis. *J. Eng. Tribol.* **1994**, *208*, 199–205.

32. Cann, P.M.; Spikes, H.A.; Hutchinson, J. The development of a Spacer Layer Imaging Method (SLIM) for mapping elastohydrodynamic contacts. *Tribol. Trans.* **1996**, *39*, 915–921.

33. Hartl, M.; Krupka, I.; Liska, M. Differential colorimetry: Tool for evaluation of chromatic interference patterns. *Opt. Eng.* **1997**, *36*, 2384–2391.

34. Leeuwen, H.V. The determination of the pressure-viscosity coefficient of a lubricant through an accurate film thickness formula and accurate film thickness measurements. *J. Eng. Tribol.* **2009**, *223*, 1143–1163.

35. Björling, M.; Larsson, R.; Marklund, P.; Kassfeldt, E. Elastohydrodynamic lubrication friction mapping—The influence of lubricant, roughness, speed, and slide-to-roll ratio. *J. Eng. Tribol.* **2011**, *225*, 671–681.

36. Bair, S.; Mary, C.; Bouscharain, N.; Vergne, P. An improved Yasutomi correlation for viscosity at high pressure. *J. Eng. Tribol.* **2013**, *227*, 1056–1060.

37. Höglund, E. Influence of lubricant properties on elastohydrodynamic lubrication. *Wear* **1999**, *232*, 176–184.

38. Bair, S. The high pressure rheology of some simple model hydrocarbons. *J. Eng. Tribol.* **2002**, *216*, 139–149.

39. Harris, K.R.; Woolf, L.A.; Kanakubo, M. Temperature and pressure dependence of the viscosity of the ionic liquid 1-butyl-3-methylimidazolium hexafluorophosphate. *J. Chem. Eng. Data* **2005**, *50*, 1777–1782.

40. Harris, K.R.; Kanakubo, M.; Woolf, L.A. Temperature and pressure dependence of the viscosity of the ionic liquids 1-methyl-3-octylimidazolium hexafluorophosphate and 1-methyl-3-octylimidazolium tetrafluoroborate. *J. Chem. Eng. Data* **2006**, *51*, 1161–1167.

41. Harris, K.R.; Kanakubo, M.; Woolf, L.A. Temperature and pressure dependence of the viscosity of the ionic liquids 1-butyl-3-methylimidazolium tetrafluoroborate: Viscosity and density relationships in ionic liquids. *J. Chem. Eng. Data* **2007**, *52*, 2425–2430.

42. Harris, K.R.; Kanakubo, M.; Woolf, L.A. Temperature and pressure dependence of the viscosity of the ionic liquids 1-hexyl-3-methylimidazolium hexafluorophosphate and 1-butyl-3-methylimidazolium BiS(trifluoromethylsulfonyl)imide. *J. Chem. Eng. Data* **2007**, *52*, 1080–1085.

43. Tomida, D.; Kumagai, A.; Qiao, K.; Yo, C. Viscosity of [bmim][PF6] and [bmim][BF4] at high pressure. *Int. J. Thermophys.* **2006**, *27*, 39–47.

44. Tomida, D.; Kumagai, A.; Kenmochi, S.; Qiao, K.; Yokoyama, C. Viscosity of 1-hexyl-3-methylimidazolium hexafluorophosphate and 1-octyl-3-methylimidazolium hexafluorophosphate at high pressure. *J. Chem. Eng. Data* **2007**, *52*, 577–579.

45. Kandil, M.E.; Marsh, K.N.; Goodwin, A.R.H. Measurement of the viscosity, density, and electrical conductivity of 1-hexyl-3-methylimidazolium bis(trifluorosulfonyl)imide at temperatures between (288 and 433) K and pressures below 50 MPa. *J. Chem. Eng. Data* **2007**, *52*, 2382–2387.

46. Pensado, A.S.; Comunas, M.J.P.; Fernández, J. The pressure-viscosity coefficient of several ionic liquids. *Tribol. Lett.* **2008**, *31*, 107–118.

47. Fernández, J.; Paredes, X.; Gacino, F.M.; Comunas, M.J.P.; Pensado, A.S. Pressure-viscosity behaviour and film thickness in elastohydrodynamic regime of lubrication of ionic liquids and other base oils. *Lubr. Sci.* **2014**, *26*, 449–462.

48. Bair, S. *High Pressure Rheology for Quantitative Elastohydrodynamics*, 1st ed.; Elsevier: Amsterdam, The Netherlands, 2007; p. 240.

49. Bair, S. A critical evaluation of film thickness-derived pressure-viscosity coefficients. *Lubr. Sci.* **2015**, *27*, 337–346.

50. Vergne, P.; Bair, S. Classical EHL versus quantitative EHL: A perspective part I—Real viscosity-pressure dependence and the viscosity-pressure coefficient for predicting film thickness. *Tribol. Lett.* **2014**, *54*, 1–12.

51. Shi, Y.; Minami, I.; Grahn, M.; Björling, M.; Larsson, R. Boundary and elastohydrodynamic lubrication studies of glycerol aqueous solutions as green lubricants. *Tribol. Int.* **2014**, *69*, 39–45.

52. Habchi, W.; Matta, C.; Joly-Pottuz, L.; Barros, M.I.D.; Martin, J.M.; Vergne, P. Full film, boundary lubrication and tribochemistry in steel circular contacts lubricated with glycerol. *Tribol. Lett.* **2011**, *42*, 351–358.